American Journal of Physics and Applications
2017; 5(6): 99-105
http://www.sciencepublishinggroup.com/j/ajpa
doi: 10.11648/j.ajpa.20170506.15
ISSN: 2330-4286 (Print); ISSN: 2330-4308 (Online)

Simulation of Multipacting with Space Charge Effect

Gennady Romanov

Fermi National Accelerator Laboratory, Batavia, Illinois, USA

Email address:
gromanov@fnal.gov

To cite this article:
Gennady Romanov. Simulation of Multipacting with Space Charge Effect. *American Journal of Physics and Applications*. Vol. 5, No. 6, 2017, pp. 99-105. doi: 10.11648/j.ajpa.20170506.15

Received: August 11, 2017; **Accepted**: September 25, 2017; **Published**: November 6, 2017

Abstract: The electron multiplication on surfaces exposed to an oscillating electromagnetic field causes the phenomenon of multipacting, which can degrade significantly the performance of vacuum RF devices, especially accelerating cavities. It is a serious obstacle to be avoided for normal operation of particle accelerator and their RF components. Many types of room temperature and superconducting accelerating cavities are designed and produced at Fermilab for different projects. The extensive simulations of multipacting in the cavities with updated material properties and comparison of the simulation results with experimental data are routinely performed during electromagnetic design of the cavities. The new advanced computing capabilities made it possible to take the space charge effect into account in the multipacting simulations. The basic new features of multipacting process that appear due to the space charge effect are shown for the classic case of the parallel plates and discussed. As the first practical application of the multipacting simulations with space charge effect the study of multipacting in the low-beta and high-beta 650 MHz elliptical superconducting cavities is also presented.

Keywords: Multipacting, Accelerator, Cavity, Secondary Emission, Space Charge

1. Introduction

Multipacting can affect practically all accelerating RF cavities and their components in the entire range energies and frequencies. Proton Improvement Plan-II [1] at Fermilab is a plan for improvements to the accelerator complex aimed at providing a beam power capability of at least 1 MW on target at the initiation of LBNE (Long Base Neutrino Experiment) operations. The central element of the PIP-II is a new 800 MeV superconducting linear accelerator, injecting into the existing Booster. A room temperature (RT) section of the linac accelerates H- ions to 2.1 MeV and creates the desired bunch structure for injection into the superconducting (SC) linac. The superconducting part of the linac explores five superconducting cavity types operating at three different frequencies. Therefore, control over the multipacting phenomena is important for this project, and as a part of overall RF design we routinely perform the extensive simulations of multipacting (MP) in each SC and RT cavity and other RF components under development (excepting SC half wave resonators since they are developed for PIP-II by other institution [2]). Also, we use every opportunity to improve overall reliability and accuracy of our simulation technique.

In present simulations with the use of CST Particle Studio we followed in general our practical approach described in [3]. Additionally, the new advanced GPU acceleration for Particle-In-Cell calculations made it possible to take space charge effect into account in this study.

It is shown in [4, 5, 6, 7] that the space charge effect plays a prominent part in the secondary electron resonance discharge, i.e. multipacting. In the elementary theory of multipacting and in the most MP simulation codes the space charge effect is neglected, which results in infinite growth of electron number in the calculations or in the simulations (a growth is typically exponential, but not always). Such MP dynamics is representative for the initial stages of multipacting development, and the multipacting thresholds predicted by the models without space charge effect usually are in a reasonably good agreement with the experiments. However, the elementary theory just cannot predict quantitative parameters of developed multipacting process such as discharge current, power, energy spectrum etc. The goal of this work was to explore the general features of the multipacting with space charge effect using simple model, then with better understanding to apply the simulation approach to the real-life case.

Parallel plates are a simplest configuration in which MP can arise, and it was used for MP theory development starting with pioneering works [8]. Many theoretical and experimental works on MP between parallel plates make this configuration a very convenient example for study and analyses. Despite the geometrical simplicity, the MP experimental results often are not in a good agreement with theory and noticeably vary depending on the emission properties, i.e. material of the plates and condition of their surfaces. Analyses of a general impact of the modern emission models on the simulation results can be found for example in [9] and will not be discussed here, though different secondary emission data will be used to fit experiments.

As a practical application of the multipacting simulations with space charge effect the study of multipacting in the PIP-II low-beta (LB, β=0.6) and high-beta (HB, β=0.9) 650 MHz elliptical superconducting cavities were performed.

2. Multipacting Between Parallel Plates

2.1. Model

A model for simulations is extremely simple – it consists of two metal rectangular plates separated by variable gap, the size of the plates depends on the gap. The fields between plates were calculated in external CST project and imported into CST PIC solver. Fields could be calculated directly in the PIC solver, because it has built-in time-domain (TD) solver, but the imported field map was used to avoid repeatable calculations of the same field during field amplitude sweep.

For the field calculation, the same model of two plates was built and used in CST TD solver. The model was equipped with two ports, and the boundaries were defined as shown in Figure 1. With two ports, it is possible to simulate field of any standing wave ratio. But pure traveling wave regime of electric field was used, since the plate sizes are much smaller than the wavelengths under interest, so the difference between TW and SW is practically negligible. The Gaussian excitation signal that is used in TD solver by default must be replaced by sinusoidal one in PIC solver (see Figure 2). PIC solver imports only instantaneous field amplitude distribution, so the length of sinusoidal signal should be long enough to reach complete multipacting development.

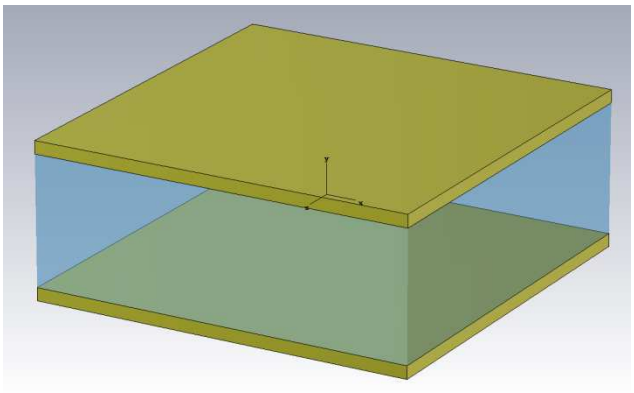

(a)

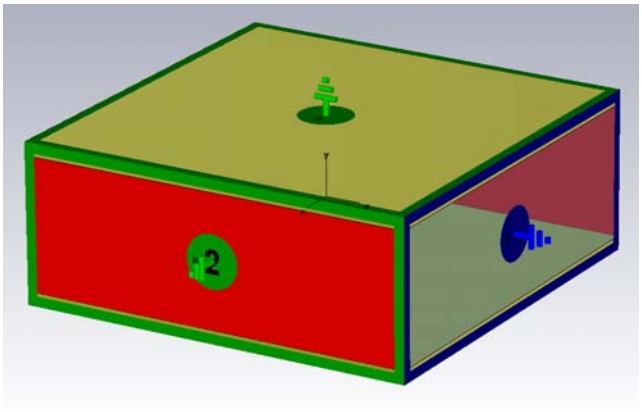

(b)

Figure 1. *a) The Model Geometry. b) The Model Boundaries: Green – Electric Wall, Blue – Magnetic Wall, Red – Waveguide Port.*

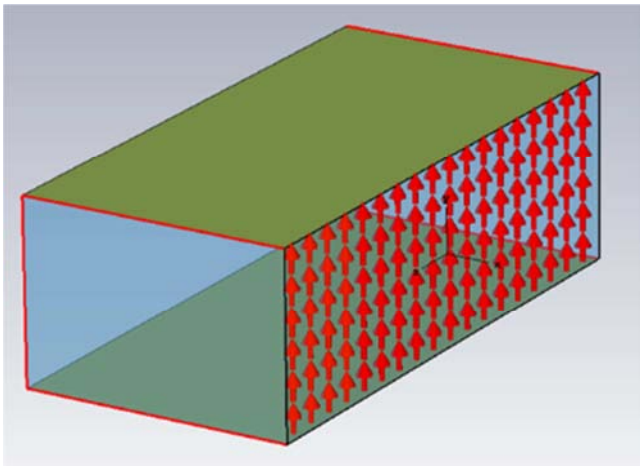

(a)

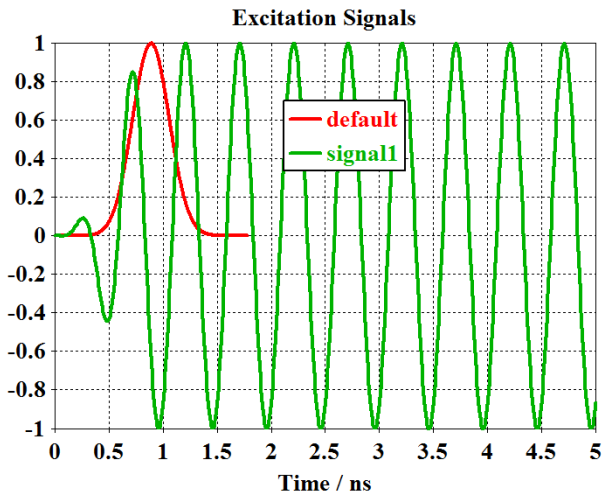

(b)

Figure 2. *a) Electric Field Distribution. b) Replacement of Default Gaussian Excitation Signal with Continuous Sinusoidal One in Time Domain Solver.*

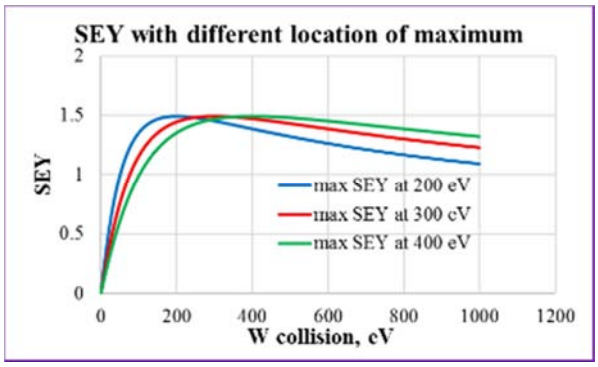

(a)

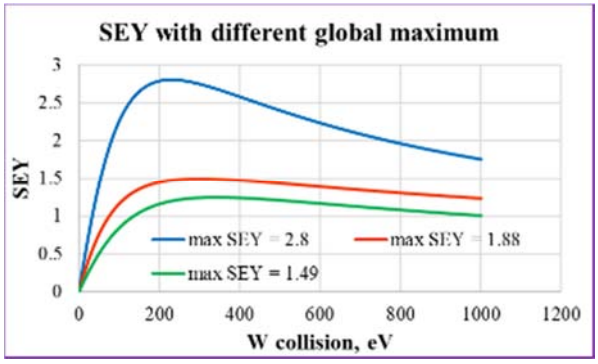

(b)

Figure 3. *SEY Functions Used in the Simulations.*

In the PIC solver, the emission properties must be assigned to the plates of the model and the initial particle sources on their surfaces must be defined.

Currently we perform PIC simulations with the use of GPU acceleration. The PIC solver with GPU acceleration does not support Furman-Pivi emission model nor any other emission model from CST PS library yet. Therefore, we had to import and use the primitive deterministic emission models in which number of secondary electrons depends only on the energy of primary electrons. The impact of elastic and diffusion scattering on the MP dynamic was considered separately at some extent in [10]. In this work, the materials with different maximal SEY and different locations of maximal SEY were considered (shown in Figure 3). The most probable initial energy of emitted electrons also changed from 0 to 7.5 eV(default).

Important advantage of the CST PIC solver are time dependent sources of initial particles, which allows distributing the initial particles over phases of RF fields. We used "Particle Area Source" with Gaussian emission model, which seems to be the most flexible and convenient for MP simulations. The details on Gaussian particle source setting are given in [11].

2.2. Multipacting of First Order

Initial parameters for the model were taken from experimental work [12]: 10 mm gap between plates and 500 MHz frequency of field between the plates. In these experiments for the plates made of copper only first order multipacting band in voltage interval of 1320-1880 V between the plates was found, which is in a good agreement with elementary theory prediction of 1786 V for first MP resonance. The PIC simulations with space charge effect just confirmed these results with the following features.

In principle developed multipacting is essentially a space charge limited process, and its first phenomena is a saturation of the discharge current density or number of particles as shown in Figure 4. During developed multipacting there are one or several bunches of electrons in RF device volume (number depends on MP order), which are well formed by phase focusing mechanism. Space charge of an electron bunch pushes peripheral particles out from phase stability interval (and possibly from area where dynamic conditions for multipacting exist). Therefore, a number of electrons continuously goes out of the game. This loss of electrons is compensated by secondary electrons re-emitted at each RF cycle. Finally, a dynamic equilibrium is established between losses and re-emission, and the process comes to the steady state regime in which discharge current density stops at certain level, and no infinite growth of particle number occurs [4, 13, 14].

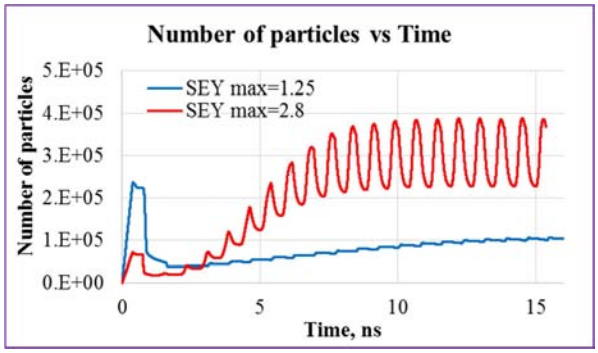

Figure 4. *Typical Behavior of Particle Number in PIC Simulations of Multipacting with Space Charge ON. Level of Particle Number Saturation Depends on Maximal SEY of Plate Material.*

Following this speculation, a discharge current density saturation level should depend on secondary emission yield of material – the higher SEY, the higher saturated current density. Indeed, one can see that in the simulations (see again Figure 4), and that was confirmed in the experiments [15]. There is also a global limit of discharge current density, which cannot be overcome at any big SEY. That is when the strength of electro-static field generated by space charge becomes comparable with driving RF field, then the interval of phase stability starts shrinking and that prevents further current density increase [14].

Direct comparison of multipacting intensity with and without space charge effect is not possible. A growth rate in saturated regime is zero, therefore it cannot be an indication of multipacting at all. An effective secondary emission yield is not a convenient indicator either, since it always equals 1 during steady multipacting regardless intensity of discharge [16]. Instead a total steady state re-emission current was used as MP characteristic in case of active space charge effect and compared with effective secondary emission yield <SEY> obtained in simulation without

space charge. The comparison resulted in the MP re-emission current and <SEY> as functions of voltage between plates shown in Figure 5.

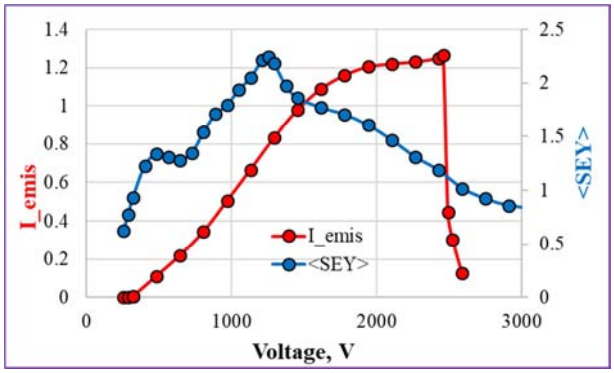

Figure 5. *Comparison of First Order MP Bands Simulated with (Red) and Without (Blue) Space Charge Effect.*

One more noticeable feature of space charge limited multipacting shown in the simulations and found in the experiments [15] is much lower energy of collision compare to the elementary theory predictions. The average energies of collisions with and without space charge can be compared directly and are shown in Figure 6. Because of that MP bands with space charge effect are shifted toward higher field levels, and they are narrower than the ones simulated without space charge [4]. Also, MP band width with space charge effect depends on maximal SEY value, which is similar to the zero-current case though (see Figure 7).

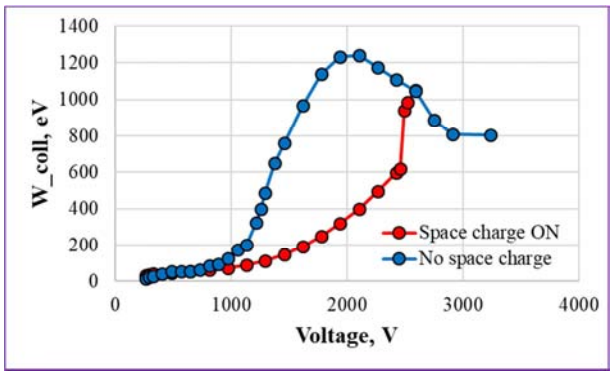

Figure 6. *Comparison of Energy of Collision in First Order MP Band.*

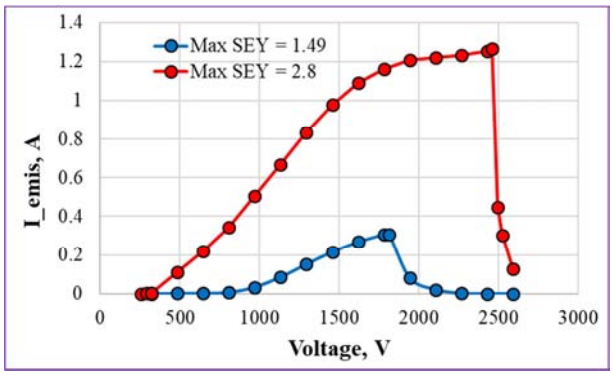

Figure 7. *First Order MP Band Simulated with Space Charge Effect and Different SEY of Plate Material.*

2.3. Multipacting of High Order Modes

For simulation of high order multipacting the model has been changed per the experiments in [17]. In these experiments three high order multipactor modes were observed in big 25.4 cm gap at frequency 50 MHz with impressive distinctness: 1st order at 10 kV, 2nd order at 3.5 kV, 3rd order at 2 kV and 4th at 1.1 kV (may be mixed with 5th).

In a big scale picture, the agreement in the mode levels between the experiments, elementary theory predictions, simulations with and without space charge looks good as shown in Figure 8 (except a resonance at ≈ 6 kV, which will be discussed later). Also, energy of collision over all bands is almost equal with and without space charge effect, possibly, a big gap matters.

The very low emission current of high order multipacting modes attracts attention. Intensity of high order modes are lower in principle due to the narrower intervals of phase stability, but not so much. The high order modes simultaneously have 2n-1 bunches of particles (or sheets, n – mode number) in a gap (see Figure 9 for example), probably, they additionally suppress re-emission and reduce total current. The multipacting mode at ≈ 6 kV is due to the existence of a peculiar resonance trajectories, described in [18] and shown in Figure 10. These trajectories have very long time of flight (≈550°) and therefore have very narrow interval of phase stability. The stable phase motion along these trajectories can exist just in case of very monoenergetic emission or sufficiently high SEY. That is why this mode was not observed in the experiments. In the simulations with Furman-Pivi emission models in which maximal SEY < 2 this mode was not observed either.

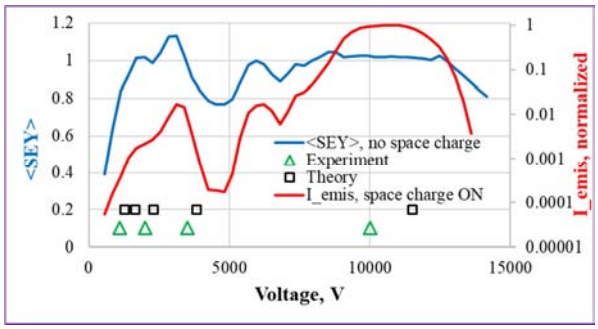

Figure 8. *Simulated, Measured and Predicted HOM Bands of Multipactor.*

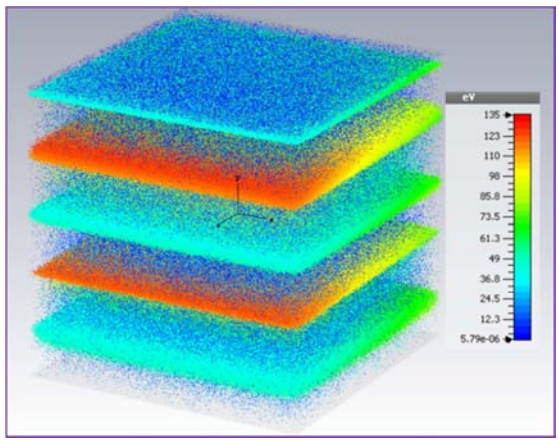

Figure 9. *Snapshot of 3rd Order Multipacting Mode. Five "Sheets" of Particles are Clearly Seen. Particle Colors Indicate Their Energy.*

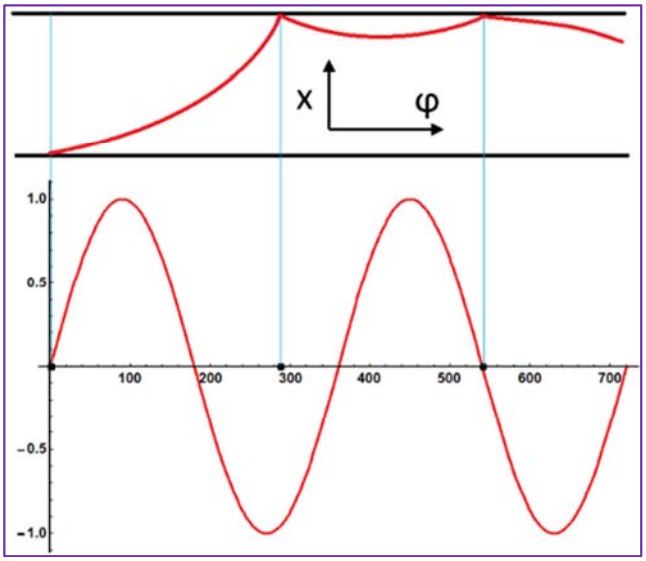

Figure 10. *A Scheme of Trajectory of "Ping-pong" Multipacting Mode in xφ Plane.*

3. Multipacting in PIP-II 650 MHz Cavities

3.1. Models and Workflow Details

The simulations were performed for the single central cells of 650 MHz cavities (the full-length models are shown in Figure 11). As usual a particular attention was given to quality of the field maps and accuracy of particle tracking which both depend strongly on mesh density. The RF field maps were calculated by CST eigenmode solver (EM) and then imported into PIC solver. In the model equator area, susceptible to MP, the minimal mesh cell size of tetrahedral mesh, which is exploited by EM solver, was 0.2 mm, while the one of hexahedral mesh used by PIC solver was 0.35 mm.

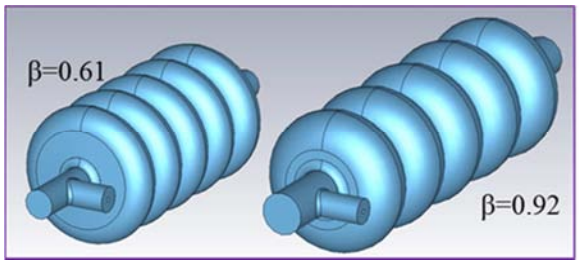

Figure 11. *The Models of PIP-II 650 MHz Cavities.*

The SEY curves used in the simulations are conventionally called "Niobium baked", "Niobium discharge cleaned" and "Niobium wet", since they are true SEY data for niobium baked at 300°C, argon discharge cleaned niobium and wet treated niobium. The limited number of simulations were performed (without GPU acceleration) with the Furman emission models to compare with. These simulations showed that for niobium the difference between probabilistic models and deterministic ones is not large, because re-emission for niobium due to the elastic and diffusion scattering is very low in the Furman models. Anyway, this discrepancy is not that important, because there is no relation to the actual condition of the cavity material, and different SEY data were used just to evaluate impact of surface finish.

3.2. Results of Simulations

How space charge effect changes MP dynamic in elliptical cavities was studied during simulations in the central cell of low beta (β=0.61) 650 MHz cavity. The multipacting with space charge ON develops in location typical for all elliptical cavities as shown in Figure 12.

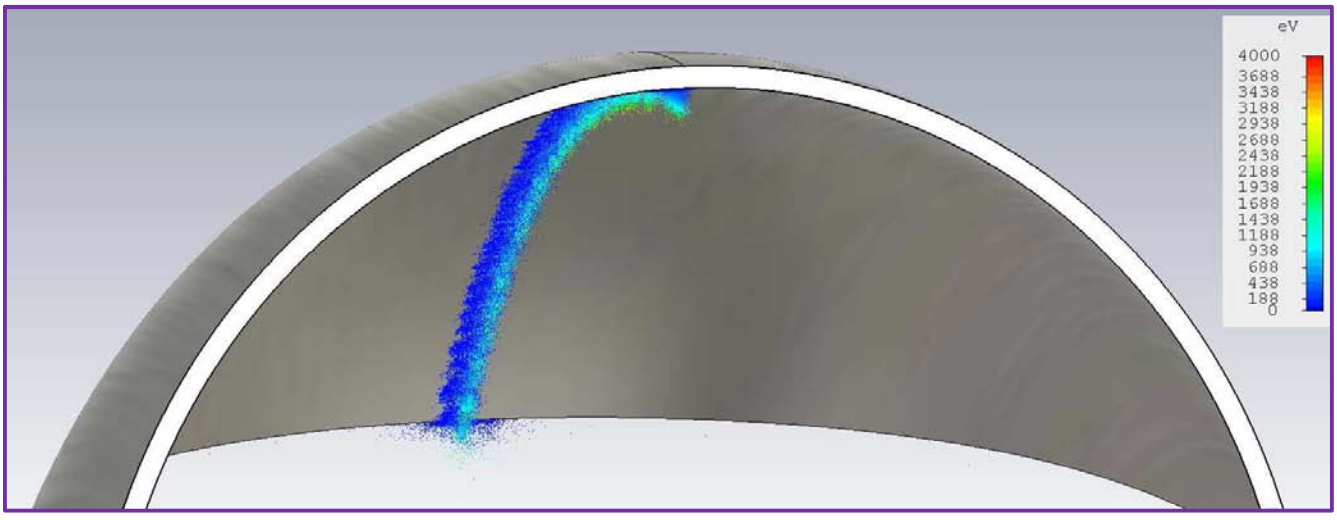

Figure 12. *Snap Shot of Steady State Multipacting with Space Charge Effect. Particle Colors Indicate Their Energy.*

The result of simulations with and without space charge effect that expresses the MP re-emission current and <SEY> as functions of cavity energy gain is shown in Figure 13. The average energies of collisions can be compared directly and are shown in Figure 14.

The result of simulation is consistent with theoretical and experimental results from [4, 14] and the simulations presented above: namely, a maximum of MP band moves

toward higher fields when space charge is ON; the MP band itself is narrower and energy of collision is lower compare to the simulations with zero space charge. But it is important to notice that the lower boundary of MP is predicted very accurately by the simulations based on the elementary theory without space charge effect.

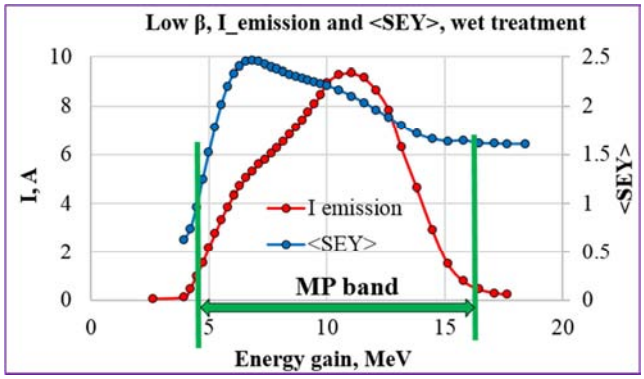

Figure 13. *Comparison of MP Simulations with Space Charge Effect (I Emission) and Without One (<SEY>).*

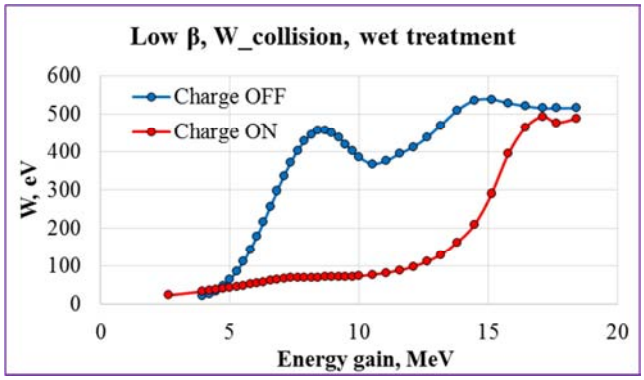

Figure 14. *Average Energy of Collisions in Simulations with Space Charge Effect and Without One.*

For both low beta and high beta models the simulations were performed with every given SEY data. The secondary emission current I_emission averaged over last 5 RF periods was calculated as the function of energy gain of a cavity. The results of simulations are presented in Figure 15-16. As contrasted to the <SEY> calculated in the simulations without space charge effect, steady state emission current in the simulations with space charge is not proportional to SEY of material, and its maximum moves toward higher fields with increasing of SEY. As it was mentioned above, the lower SEY, the closer the results obtained with and without space charge effect, since MP steady state regime is achieved at smaller space charge for low SEY.

In general, the present results are in a good consistency with the previous simulations and experiments. The MP barrier in the low beta single cell simulated in [19] with Furman-Pivi SEY model is 4.9÷11.4 MeV. The experiments with single low beta cells in [20] demonstrated the MP activity in 4.9÷5.6 MeV interval - apparently, the cells were clean enough and RF conditioning eliminated the MP barrier very quickly. The power tests of 5 cell high beta cavity at Fermilab [21] had the MP problems in the interval of 10.6÷17 MeV.

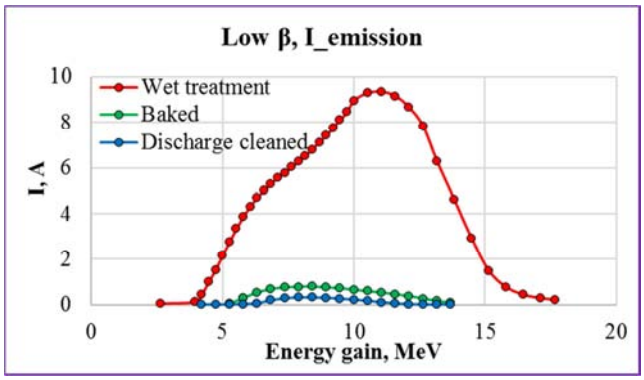

Figure 15. *Average Energy of Collisions in Simulations with Space Charge Effect and Without One.*

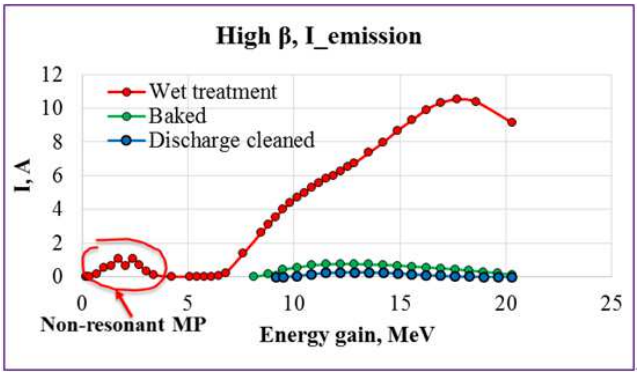

Figure 16. *Average Energy of Collisions in Simulations with Space Charge Effect and Without One.*

4. Conclusion

The inclusion of space charge effects in MP simulations does not result in significant changes in the location MP barriers compare to the simulations without space charge. On the other hand, a width of MP barrier may be overestimated without space charge. The energy of collision and the power deposition in the simulations with space charge effect are lower compare to the classic theory.

References

[1] Proton Improvement Plan, website: http://www-ad.fnal.gov/proton/PIP/PIP_index.html.

[2] Z. A. Conway et al, "Achieving High Peak Fields and Low Residual Resistance in Half-Wave Cavities", in Proc. SRF'15, Whistler, BC, Canada, 2015, paper WEBA05, pp. 973-975.

[3] Gennady Romanov, Paolo Berrutti and Timergali N. Khabiboulline, "Simulation of Multipacting in SC Low Beta Cavities at FNAL", in Proc. IPAC'15, Richmond, Virginia, USA, 2015, paper MOPMA018, pp. 579-581.

[4] D. K. Callebout, "Secondary Electron Resonance Discharge: I. Steady State by Debunching", Physica, Issue 7, July 1963, pp. 784-802.

[5] C. J. Lingwood et al, "Phase space analysis of multipactor saturation in rectangular waveguide", Physics of Plasmas 19, 032106 (2012).

[6] M. Buyanova et al, “Influence of secondary emission yield on the saturation properties of multipactor discharges between two parallel metal plates”, Physics of Plasmas 17, 043504 (2010).

[7] E. Sorolla and M. Mattes, “Multipactor saturation in parallel-plate waveguides”, Phys. Plasmas 19, 072304 (2012).

[8] A. J. Hatch and H. B. Williams, “Multipacting Modes of High-Frequency Gaseous Breakdown”, The Physical Review, 2nd series, Vol. 112, No. 3, November 1, 1958.

[9] R. Seviour, “The Role of Elastic and Inelastic Reflection in Multipactor Discharges”, IEEE Trans. on Electron Devices, vol. 54, No 8, August, 2005.

[10] G. Romanov, «Stochastic Features of Multipactor in Coaxial Waveguides for Travelling and Standing Waves», preprint PUB-11-003-TD, Fermilab, Batavia, IL 60510, USA, 2011.

[11] P. Berutti, T. Khabiboulline, G. Romanov, «Multipactor Discharge in the PIP-II Superconducting Spoke Resonators», Fermilab, Technical division, Technical note TD-16-005, 2016.

[12] D. Proch, D. Einfeld, R. Onken, and N. Steinhauser, “Measurement of multipacting currents of metal surfaces in RF fields”. WPQ24, IEEE Proceedings, PAC 95, 1776, 1996.

[13] Liao Lang et al, “Multipacting Saturation in Parallel Plate and Micro-Pulse Electron Gun”, Chinese Phys. C, Volume 39, Number 2, March 2014.

[14] Волков В. А., Ганичев Д. А., «Стационарное состояние вакуумного вторично-эмиссионного ВЧ разряда», Журн. техн. физ., 1982, т. 52, № 8, с. 1559-1563.

[15] Ганичев Д. А., Станский В. А., Фридрихов А. С., «Экспериментальное исследование эмиссии вторичных электронов на свервысоких частотах», Изв. АН СССР, Сер. физ., 1971, т. 3 5, № 2, с. 268-269. 1982, т. 52, № 8, с. 1559-1563.

[16] S. Riyopoulos, D. Chernin, D. Dialetis, “Theory of Electron Multipactor in Crossed Fields”, Physics of Plasmas, Issue 8, Volume 2, 1995, pp 3194 - 3213.

[17] C. W. Hoover, Jr., and R. K. Smither, "Secondary Electron Resonance Discharge Mechanism”, Phys Rev. 98, 1149, (1955).

[18] M. Siddiqi, R. Kishek, “Simulation of Ping-Pong Multipactor With Continuous Electron Seeding”, in Proc. NA-PAC’16, Chicago, IL, USA, 2017, paper MOPOB53, pp. 181-183.

[19] S. Kazakov, I. Gonin and V. P. Yakovlev, “Multipactor Simu-lation in SC Elliptical Shape Cavities”, in Proc. IPAC’12, New Orleans, Virginia, USA, 2012, paper WEPPC051, pp. 2327-2329.

[20] F. Marhauser et al, “Design, Fabrication and Testing of Me-dium-Beta 650 MHz SRF Cavity Prototypes for Project-X”, in Proc. IPAC’11, San Sebastián, Spain, 2011, paper MOPC114, pp. 343-345.

[21] V. P. Yakovlev, private communication, April 2016.